26th ABCM International Congress of Mechanical Engineering
November 22-26, 2021. Florianópolis, SC, Brazil

COB-2021-1041
NUMERICAL STUDY OF THE RELATIONSHIP BETWEEN THE LOAD APPLIED BY THE BOLT AND THE STRESS INTENSITY FACTOR IN A MODIFIED-WOL SPECIMEN

Emerson da Trindade Marcelino
Jorge Antonio Palma Carrasco
Nadège Sophie Bouchonneau da Silva
José Maria Andrade Barbosa
Universidade Federal de Pernambuco, Department of Mechanical Engineering, Av. da Arquitetura, s/n, Cidade Universitária, Recife – PE – Brazil, 50740-550
emerson.trindadem@ufpe.br; jorge.carrasco@ufpe.br; nadege.bouchonneau@ufpe.br; jose.mabarbosa@ufpe.br

Abstract. *The Modified-WOL specimen is a compact, bolt-loaded device used for fracture toughness tests of engineering materials in environment-assisted conditions, which provides the Threshold Stress Intensity Factor for Environment-Assisted Cracking, K_{IEAC}, value with one specimen only. Its internal bolt yields a constant notch opening, requiring a clip gauge to measure this displacement inside the environmental chamber to calculate the initial K_I applied. However, corrosion reactions with the environmental solution limits the use of clip gauge. So, this work aims to propose a method for the specimen's setup based on a correlation between the load applied by bolt and the K_I by three- and bi-dimensional simulations with the Finite Element Method. With the three-dimensional simulation, we obtained the corresponding load reactions and opening displacements for each bolt rotation. From these results, we did theoretical K_I calculations. With those load values, bi-dimensional simulations were performed to obtain numerical K_I and validate the three-dimensional modeling. We obtained correlation equations from the numerical results to estimate the amount of bolt rotation and bolt load needed to apply a desired value of K_I at the crack front. The results indicated that the numerical model used is appropriate to simulate the specimen's setup, achieving acceptable errors.*

Keywords: *Modified-WOL specimen, Bolt-loaded specimen, Finite Element Method, Environment-Assisted Cracking.*

1. INTRODUCTION

Characterizing the fracture toughness of engineering materials that work in aggressive environments is essential for the mechanical design and maintenance of structures and structural elements. The experimental determination of fracture toughness in environment-assisted conditions is expensive because the test method currently used in laboratories requires multiple specimens and long test times. An alternative test method is the constant displacement fracture toughness test performed with the Modified Wedge Opening Load (Modified-WOL) specimen, standardized by ASTM E1681-03 (2020). The Modified-WOL specimen has the main advantage of providing the value of the Threshold Stress Intensity Factor for Environment-Assisted Cracking (K_{IEAC}) with one specimen only (Anderson, 2005). This specimen has an internal bolt and a reaction pin as the loading device, therefore not needing a tensile testing machine, resulting in a compact system, and easy-to-be-used.

The bolt imposes an initial load for the constant crack opening when a pre-cracked Modified-WOL specimen test setup is used. A clip gauge measures the crack mouth opening displacement that will be used to calculate the initial Mode I Stress Intensity Factor (K_I). This initial K_I value must be lower than the Fracture Toughness (K_{Ic}) of the material. As the test goes, a relaxation of the load applied by the bolt due to crack propagation occurs, but the crack mouth opening displacement should remain constant. The test instrumentation records this load relaxation by time and calculates instantaneous K_I values. This monitoring will indicate when the K_I decreases until reaching a constant value, which will occur when the crack arrests, whose value will correspond to the threshold for K_{IEAC} of the test (Chung *et al.*, 1985; Vigilante *et al.*, 2000; Tjayadi *et al.*, 2020).

Preconditioning of the Modified-WOL specimen in the environment before displacement application will greatly influence the resulting K_{IEAC} values (ASTM, 2020). Thus, ASTM E1681-03 (2020) guides that the specimens shall be pre-exposed to the environmental solution immediately preceding the test for at least 10% of the total test time, or 8h. Then, the bolt loads the specimen, measuring the amount of applied crack mouth opening displacement with a clip gauge for the initial K_I calculation. However, ASTM E1681-03 (2020) advises that using a clip gauge is limited due to corrosion reactions that may occur between the clip gauge and the test specimen when this gauge is placed directly above or into

an environmental chamber. So, to guide the test setup in this condition, could we use a correlation between the load applied by the Modified-WOL specimen's bolt and the applied K_I?

Therefore, to allow the Modified-WOL specimen's setup without requiring a clip gauge, this work aims to propose a setup method based on a correlation between the load applied by the bolt due to its rotation and the applied K_I. To obtain this correlation, we will simulate with Finite Element Method (FEM) three- and bi-dimensional models of this system composed of the specimen, the bolt, and the reaction pin. The objective of the three-dimensional simulation is to obtain the load reactions and crack mouth opening displacements corresponding to each bolt rotation angle. After that, calculations with each notch opening displacements using the equation from ASTM E1681-03 (2020) will result in theoretical K_I values. Furthermore, with the load reactions, bi-dimensional simulations will be done to obtain numerical K_I values for comparison with these theoretical calculations. This work is organized as follows: Section 2 explains the method followed on this work for the numerical modeling and calculations; Section 3 presents the results and discusses the central points of the work; in Section 4, the main conclusions and limitations of the work are presented; and Section 5 concludes this document with the authors' acknowledgments.

2. NUMERICAL SIMULATIONS

This section presents the steps followed in carrying out the three- and bi-dimensional computational simulations via FEM. Firstly, we present the mechanical properties of the steels adopted in both analyses. Then, we describe the three- and bi-dimensional geometries, numerical modeling, and K_I calculations.

2.1 Material properties

The materials adopted in both analyses had homogeneous, isotropic, and linear-elastic behavior. The API 5L steel grade X70 was adopted for the specimen. It is a High Strength Low Alloy (HSLA) steel for pipelines standardized by API (2018). Moreover, the bolt and the reaction pin were modeled with 17-4-PH (H900) martensitic stainless-steel precipitation hardened, based on those used by Chung *et al.* (1985) and Vigilante *et al.* (2000). Table 1 lists the mechanical properties of these steels based on the API (2018) and NAS (2021).

Table 1. Mechanical properties of the steels adopted in three- and two-dimensional analysis.

	Elastic Modulus (E) [Pa]	**Poisson's Ratio (ν) -**	**Yield Stress (σ_y) [Pa]**	**Ultimate Tensile Stress (σ_{UT}) [Pa]**
API 5L X70	2.10×10^{11}	0.3	4.85×10^{8}	5.70×10^{8}
17-4-PH (H900)	2.10×10^{11}	0.3	1.172×10^{9}	1.31×10^{9}

2.2 Three-Dimensional Analysis

In this subsection, we describe the three-dimensional static structural analysis of this problem. Initially, we present the geometry of the system components following the recommendations of the ASTM E1681-03 (2020) standard. Then, we show the analysis modeling considering the non-linear frictional contacts and definition of Boundary Conditions. To finish this subsection, we present the equations from ASTM E1681-03 (2020) used for the theoretical calculation of K_I with the results from this three-dimensional analysis.

2.2.1 Geometries

For the K_{IEAC} test results to be valid, the specimen should have predominantly elastic behavior and the Plane Strain condition be met (ASTM, 2020). Therefore, specimen thickness B, the initial crack length a_0, and ligament size $(W - a_0)$ should be chosen based on the minimum specimen's size requirements calculated with Eq. (1). So, replacing the material properties of API 5L X70 steel presented in Table 1 on Eq. (1), the size requirements calculated for this condition are $B, a0, (W - a0) \geq 5.77$ mm. Considering that this specimen would be hypothetically machined from a commercial tube (Vallourec, 2021) with an outer diameter of 298.5 mm (11 ¾ in) and a wall thickness of 14.78 mm (0.582 in), we adopted the best specimen thickness of B = 12.7 mm (1/2 in).

$$B,\ a_0,\ (W - a_0) \geq 2{,}5\frac{\sigma_y}{E}, \tag{1}$$

Observing that the dimensions of the specimen, the bolt, and the reaction pin, according to ASTM E1681-03 (2020), are defined as functions of the specimen's width W, which is equivalent to twice the thickness previously adopted, we created the three-dimensional geometries shown in Figure 1. A geometrical straight crack was created at the notch front

with a sharpening angle of 1º and 0.02 mm opening to simulate the pre-crack. ASTM E1681-03 (2020) also specifies the thread type, which must be of the Fine Serie of Unified Inch Threads (UNF) standardized by the ASME B1.1 (2019). So, we see from Figure 1 that for the nominal diameter of 6.35 mm, the UNF thread has 28 threads per inch, which corresponds to a pitch of approximately 0.907 mm (0.0357 in).

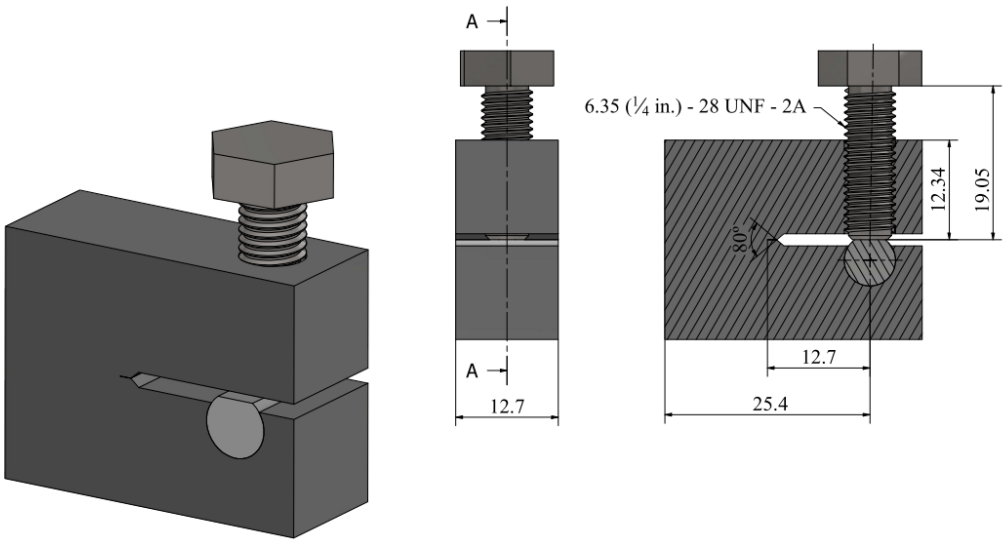

Figure 1. Isometric, front, and side cut views of the Modified-WOL's assembly, with dimensions in millimeters.

2.2.2 Analysis modeling

The modeling of this analysis consists of the configuration of non-linear contacts, the definition of the cylindrical joint, the application of Boundary Conditions, and Mesh generation. Firstly, the Augmented Lagrangian method was adopted as the non-linear contact formulation between the three contact pairs of this system due to a reasonable penetration control between the contact surfaces that ensures better numerical stability. (Vilela *et al*., 2019; Vilela, 2016; ANSYS, 2004; Telega and Gałka, 2001; Bandeira *et al*., 2010). Vilela *et al*. (2019) explains that with this method, the forces developed in this region are decreased so that the penetration resulting from the contact between parts does not exceed the allowed limit value. The Augmented Lagrangian method is the most used to solve mechanical contact problems with high pressures at the contact interfaces (Bandeira *et al.*, 2010). The contact pairs of this system are shown in Figure 2(A): 1st Contact Region) Between the bolt and the flat surface of the reaction pin, indicated by *a* in Figure 2(A); 2nd Contact Region) Between the bolt's and specimen's threads, indicated by *b* in Figure 2(A); and 3rd Contact Region) Between the curved surfaces of the reaction pin and the specimen, indicated by *c* in Figure 2(A). For these three contact pairs, the coefficient of friction μ considered was 0.42, a reference value for a case of dynamic friction between two dry surfaces of hard steels (Avallone *et al.*, 2007).

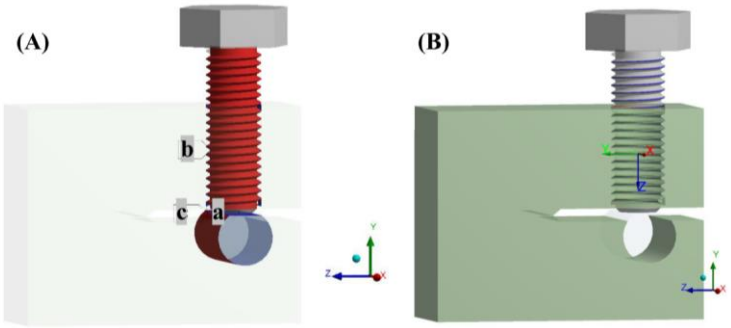

Figure 2. (A) Indications of the three frictional contact pairs of the system; And (B) Cylindrical joint between the specimen's hole and the bolt.

A deformable cylindrical joint was defined between the threads of the Modified-WOL specimen and the bolt, shown in Figure 2(B). Thus, 2 Degrees of Freedom were allowed for the bolt's motion, which are the rotation and translation about the Z-axis of the Local Coordinate System, that has the same direction of the longitudinal axis of the bolt.

Due to the large rotation angles that the bolt may suffer in a laboratory test setup, the application of the Boundary Conditions was divided into four static load-steps with automatic sub-steps for gradual transitions. Constant displacement constraints in the three directions of the Global Reference System were applied on the specimen's edge indicated by *A* in Figure 3. On edge indicated by B, constraints were applied only on X and Z directions, and free displacement in Y. Those constraints were necessary to avoid rigid body motion due to the reactions on the frictional contacts and enable solution convergence. Rotation angles (α) of 45º clockwise were applied to the bolt in each load-step with gradual sub-step increments, reaching 180º. A mesh with 290,866 nodes and 196,279 elements was generated with SOLID187 at the specimen and the bolt and SOLID186 at the pin.

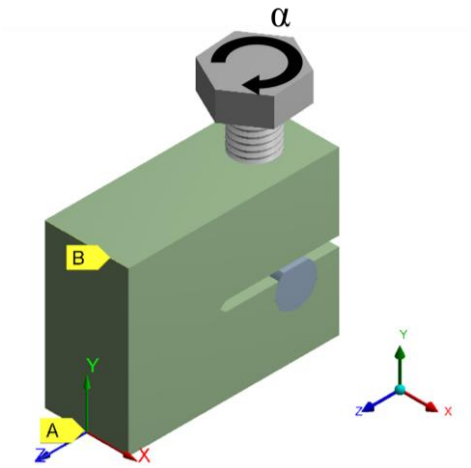

Figure 3. System's Boundary Conditions.

2.2.3 Theoretical K_I Calculation

With the results of this three-dimensional analysis, theoretical K_I values were calculated based on Eq. (2) from ASTM E1681-03 (2020). From this equation, a/W is the ratio between the crack length and the specimen width, $f(a/W)$ is the correction factor given by Eq. (3), and the crack mouth opening displacement V was obtained by this three-dimensional analysis as illustrated by Figure 4.

$$K_I = \frac{VE}{\sqrt{W}} f\left(\frac{a}{W}\right), \tag{2}$$

$$f\left(\frac{a}{W}\right) = \left(1 - \frac{a}{W}\right)^{1/2} \left[0.654 - 1.88\left(\frac{a}{W}\right) + 2.66\left(\frac{a}{W}\right)^2 - 1.233\left(\frac{a}{W}\right)^3\right], \tag{3}$$

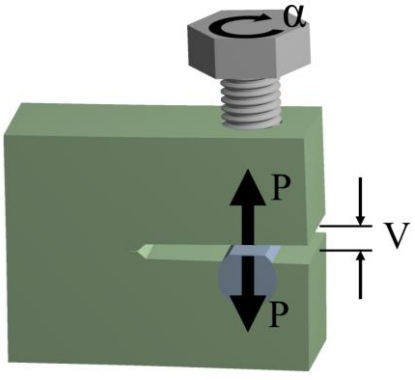

Figure 4. Parameters obtained from the three-dimensional simulation results.

2.3 Bi-Dimensional Analysis

This subsection describes the bi-dimensional analysis to validate the three-dimensional model by calculating the K_I values numerically for different contact reaction forces as Boundary Conditions. Firstly, we present the bi-dimensional

geometry adopted for this analysis. Then, we show the Boundary Conditions, mesh element type, and numerical K_I calculation.

2.3.1 Geometry

These bi-dimensional analyses were performed using half of the Modified-WOL specimen geometry presented in Figure 1 before. Figure 5 presents this geometry. A sharp and straight half-crack was also assumed in this model, as shown in detail *B* in Figure 5. For the K_I calculation, the linear-elastic material behavior was used as the constitutive law, with the parameters *E* and *v* taken from Table 1. Also, the Plain Strain condition was considered.

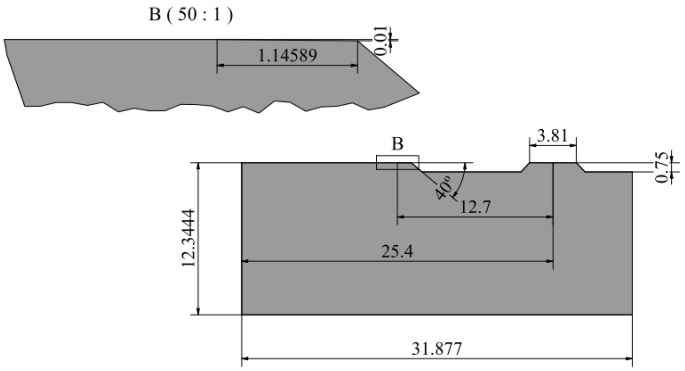

Figure 5. Bi-dimensional geometry of the Modified-WOL with dimensions in millimeters.

2.3.2 Analysis Modeling and Numerical K_I Calculation

The Boundary Conditions were applied to this model, as shown in Figure 6, which were the displacement restriction at one vertex, the symmetry line at the ligament region, and the distributed force *P* at the surface nodes of the reaction pin. This force *P* is due to reaction loads at the Bolt-Pin Contact Region shown in Figure 4 before, obtained from the three-dimensional simulation.

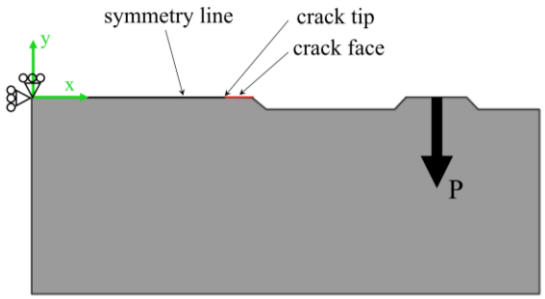

Figure 6. Boundary Conditions of bi-dimensional analysis.

Figure 7 shows the mesh generated with 18,068 nodes and 5,947 elements of type 8-node PLANE183 and, in more detail, the distributed force *P* applied on the surface nodes of the pin. Quarter-point singular elements were used at the half-crack tip to enhance numerical accuracy for K_I calculation (Anderson, 2005), while the other parts of the model used quadrilateral elements.

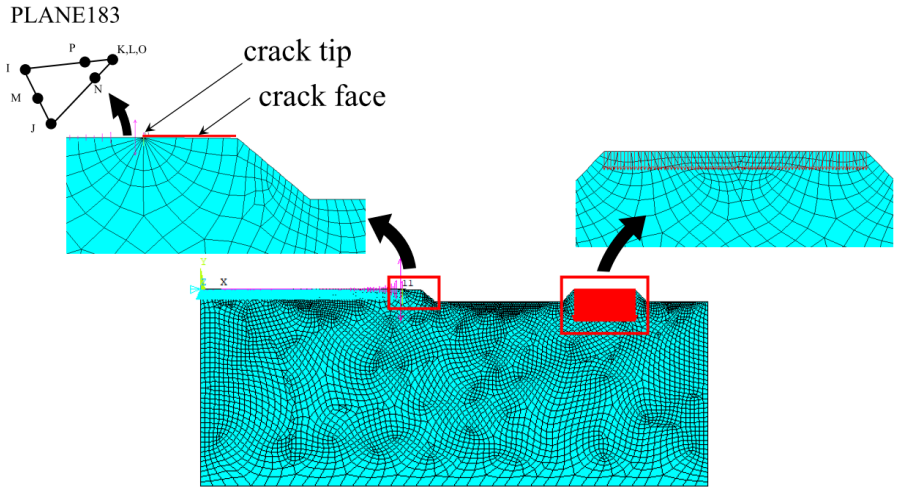

Figure 7. Mesh configuration and Boundary Condition in detail.

Finally, to calculate KI numerically, a three-point path at the crack face was defined for the Approximate Crack-Tip Displacements method calculation based on the nodal displacements in the vicinity of the crack, as indicated in Figure 8. Equation (4), from ANSYS (2018), shows this K_I calculation for a half-crack model, where G is the shear modulus, $\kappa = 3-4\upsilon$ for Plane Strain, and $\frac{|v|}{\sqrt{r}}$ is the factor based on the nodal displacements and locations.

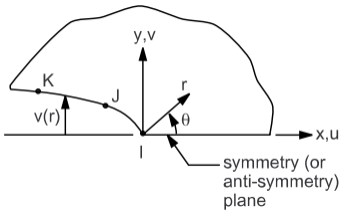

Figure 8. Nodes used for the Approximate Crack-Tip Displacements method, from ANSYS (2018).

$$K_I = \sqrt{2\pi}\frac{2G}{1+\kappa}\frac{|v|}{\sqrt{r}}, \tag{4}$$

3. RESULTS AND DISCUSSION

Figure 9 shows the average crack mouth opening displacements measured from the three-dimensional simulation due to the specimen's deformation for each bolt rotation and their corresponding theoretical K_I calculated according to Eqs. (2) and (3) from ASTM E1681-03 (2020).

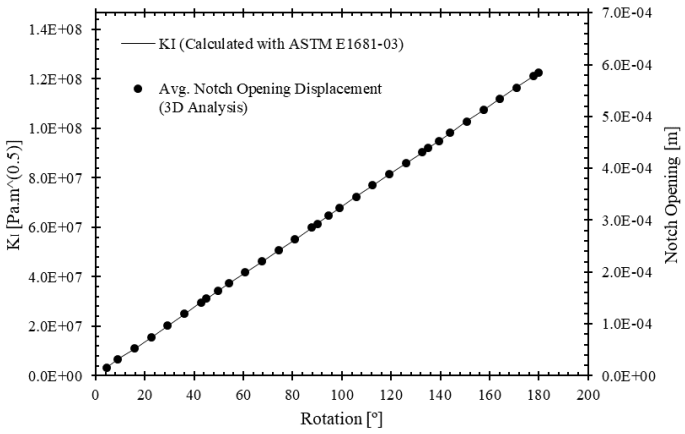

Figure 9. Crack mouth opening displacements and theoretical K_I calculated for each bolt rotation.

Figure 10 shows in three different projection views the resultant reaction force vectors at the Bolt-Specimen Contact Region and at the Bolt-Pin Contact Region that arose on the specimen and the pin, respectively, due to the bolt loading. We note that at both contacts, the reaction force vectors are not parallel to plane YZ of the Global Coordinate System, even with perfect contacts between the surfaces of these components that were established by contact constraints during the assembly of this geometry and without misalignments.

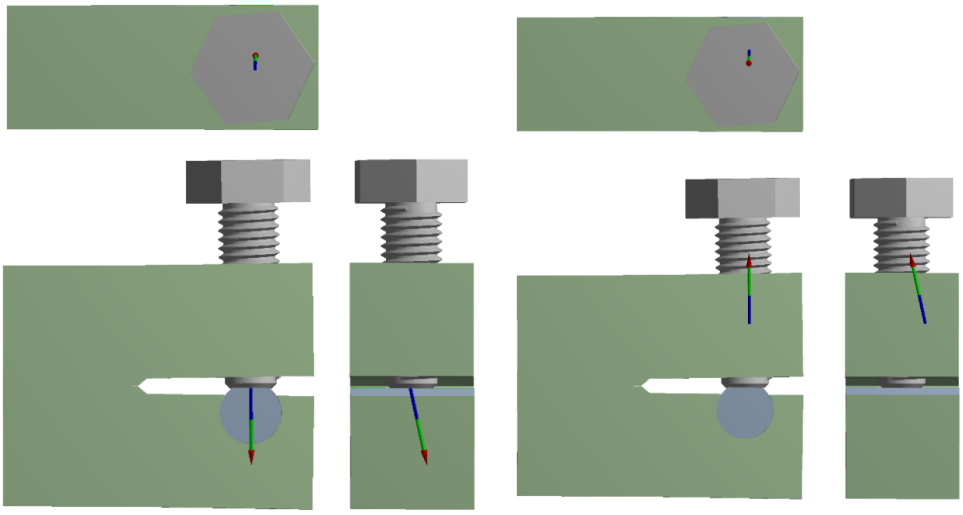

Figure 10. Views of the resultant reaction force vectors at Bolt-Specimen Contact (Left) and Bolt-Pin Contact (Right).

We obtained these two resultant reaction forces for each bolt rotation, whose values Figure 11 shows. Not counting the resultant reaction forces at those two contact regions at 4.5º bolt rotation, which had a difference of 522.60 N between them, from the second point onwards, this difference was reduced to an average of 0.50 N ± 0.50 N. Also, in Figure 11, two linear correlation equations were presented to estimate the reaction forces based on the angle of bolt rotation α. They are shown in Eq. (5) for the reaction force $P_{(1)}$ at the Bolt-Pin Contact Region and in Eq. (6) for the reaction force $P_{(2)}$ at the Bolt-Specimen Contact Region.

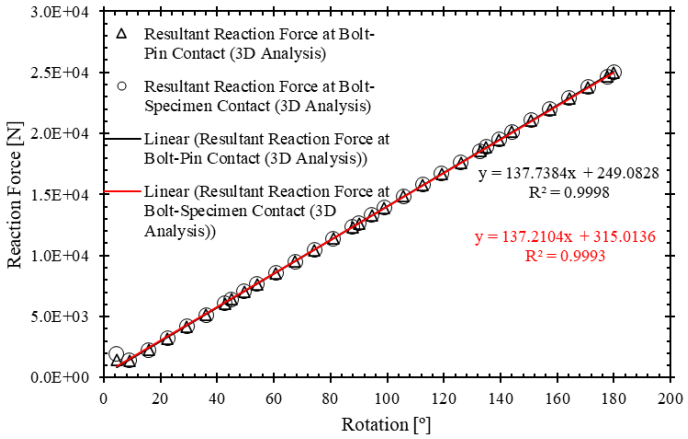

Figure 11. Reaction forces from Bolt-Pin and Bolt-Specimen Contact Regions and interpolation functions.

$$P_{(1)}=137.7384\alpha + 249.0828, \quad (5)$$

$$P_{(2)}=137.2104\alpha + 315.0136, \quad (6)$$

With these resultant reaction forces obtained at the Bolt-Pin Contact Region, the force Boundary Conditions were applied to the nodes of the bi-dimensional model as explained in subsection 2.3 to calculate numerical K_I values. Figure 12 presents these results, where linear interpolation gave us Eq. (7) that associates the resultant reaction force $P_{(1)}$ at the Bolt-Pin Contact Region with the K_I at the crack tip.

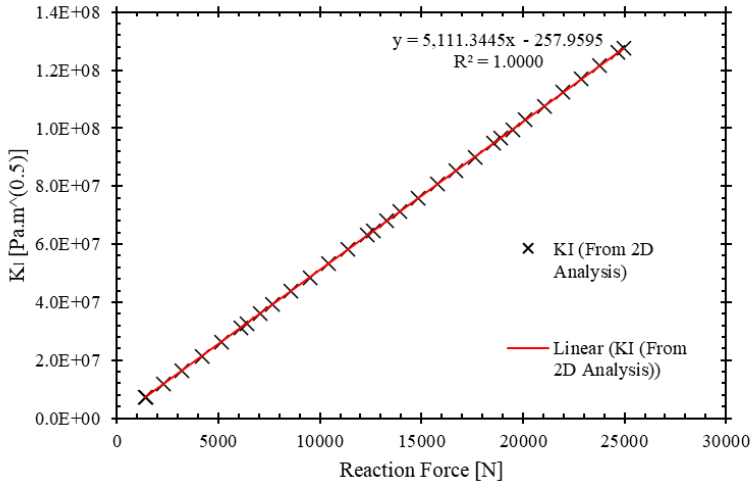

Figure 12. Numerical K_I by each reaction force and interpolation function.

$$K_I = 5,111.3445P_{(l)} - 257.9595, \quad (7)$$

Figure 13 shows the comparison results between these numerical K_I values obtained by the bi-dimensional analysis and those previously calculated by Eqs. (2) and (3), and the relative errors calculated. As observed before, with the first reaction force corresponding to 4.5º, the first numerical K_I value was significantly higher than in theory, with an error of 121.00%. However, this error was reduced significantly from the second point onwards.

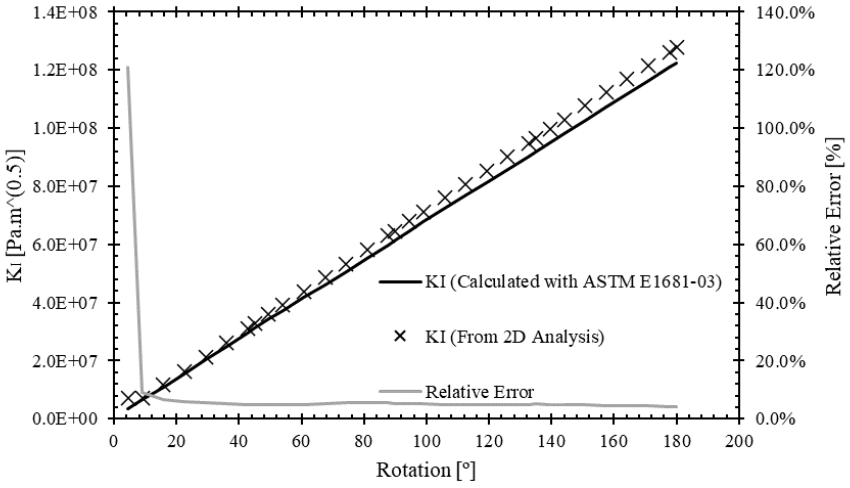

Figure 13. Numerical and theoretical K_I values and the curve of relative error.

For a closer analysis of these errors obtained in Figure 13, Figure 14 shows the boxplot displaying the distribution of these values. Figure 14 gives that 50% of the relative errors lie in the range of 4.87% and 5.38%, with an average value of 4.99%. The minimum and maximum values obtained are 4.20% and 6.02%. Furthermore, the errors 121.00%, 8.97%, and 6.58%, which corresponds to the rotations of 4.5º, 9º, and 15.75º, are the outliers of this boxplot.

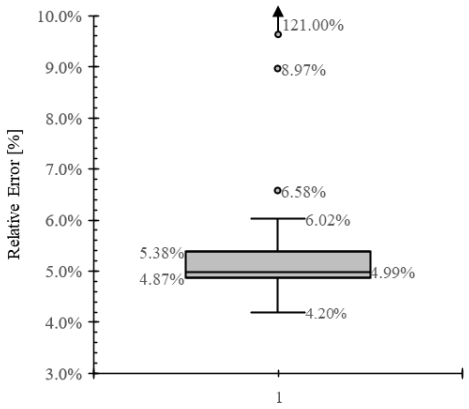

Figure 14. Generated boxplot with the relative errors between numerical and theoretical K_I values.

To complete this section, Figure 15(A) presents the von-Mises stress fields at the cross-section plane in the three-dimensional specimen model at 22.5º bolt rotation. Figure 15(B) shows the von-Mises stress fields at the bi-dimensional model with the corresponding resultant force reaction at the Bolt-Pin Contact Region at 22.5º bolt rotation, which is 3,209.2 N, applied as the Boundary Condition. Figure 15(C) shows the von-Mises stress fields at the cross-section of the complete three-dimensional model, with the specimen, the bolt, and the pin.

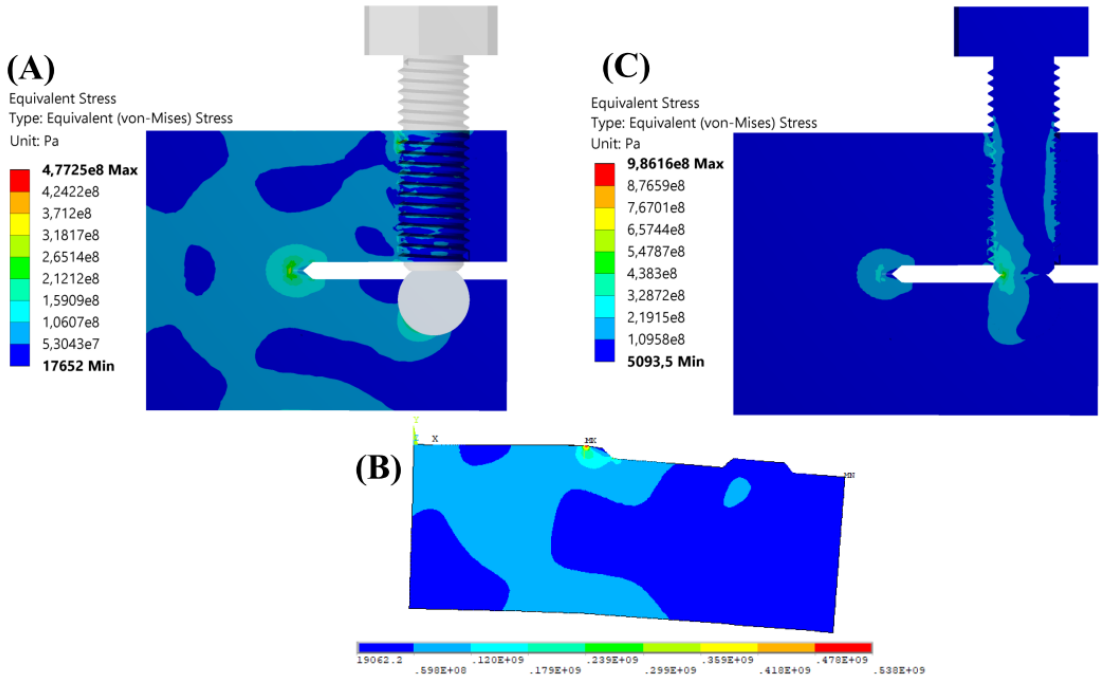

Figure 15. Von-Mises stress fields in (A)Three-dimensional specimen model; (B) Bi-dimensional model; And (C) Three-dimensional complete model.

4. CONCLUSION

In this work, we performed three- and bi-dimensional Finite Element simulations of the Modified-WOL specimen to obtain a correlation between the bolt rotation, the reaction load on this bolt, and the initial K_I applied to the specimen. The objective of the three-dimensional simulation was to obtain the load reactions and crack mouth opening displacements corresponding to each bolt rotation angle. After that, we calculated theoretical K_I values with each crack mouth opening displacements using an equation from ASTM E1681-03 (2020). Bi-dimensional simulations were done with these load reactions to obtain numerical K_I values for comparison with theoretical calculations.

Thus, the simplifications adopted in the bi-dimensional analysis, which were the symmetrical geometry and the homogeneous force distribution at the Boundary Condition, gave us acceptable numerical K_I approximations. In addition, hardware limitations for further mesh refinements at the three-dimensional analysis and the FEM approximations to

calculate the crack mouth opening displacements and the reaction forces for each bolt rotation contributed to the accumulation of errors. Further works could be done with finer mesh at the three-dimensional model and apply a variable force distribution as the Boundary Condition of the bi-dimensional model, as observed by the stress distribution at the Bolt-Pin Contact Region in Figure 15(C), to minimize these errors.

Despite that, the numerical and theoretical proximate results of K_I obtained in this work corroborate that the method followed for the three-dimensional analysis modeling is appropriate to simulate the test setup of the Modified-WOL specimen. Also, we can use the reaction force measured at the Bolt-Pin Contact Region to calculate the applied K_I at the crack front with Eq. (7) obtained by linear interpolation of Figure 12 for the geometry size and materials adopted in this work. In addition to this, Eqs. (5) and (6), obtained by linear interpolation of Figure 11, can be used to calculate the reaction forces at the Bolt-Pin Contact Region and the Bolt-Specimen Contact Region, respectively, based on the applied bolt rotation. Therefore, with these equations, we can calculate the amount of bolt rotation needed to apply a desired value of K_I at the crack front of the Modified-WOL specimen, and thereby this angle of rotation applied to the bolt can be controlled by measuring it with a torsion angle gauge, for example.

5. ACKNOWLEDGEMENTS

This study was financed in part by the Coordenação de Aperfeiçoamento de Pessoal de Nível Superior – Brasil (CAPES) – Finance Code 001. The Postgraduate Program in Mechanical Engineering from UFPE also supported this work.

The first author thanks Prof. Kyller Costa Gorgônio from UFCG and Prof. Adson Diego Dionísio da Silva from IFPB for their technical support and Dr. Anderson da Trindade Marcelino for his recommendations.

6. REFERENCES

Anderson, T.L., 2005. *Fracture Mechanics - Fundamentals and Applications*. 3rd ed. Vol. 1. Londres: Taylor & Francis Group.

ANSYS, 2018. “17.7. POST1 - Crack Analysis.” 2018.

ANSYS, 2004. *Contact Technology Guide*. *Contact Technology Guide*.

API, 2018. “API Specification 5L - Line Pipe, 46th Edition.,” no. 46.

ASME, 2019. “ASME B1.1: Unified Inch Screw Threads (UN and UNR Thread Form).” ASME International.

ASTM, 2020. “ASTM E1681-03: Standard Test Method for Determining Threshold Stress Intensity Factor for Environment-Assisted Cracking of Metallic Materials.” *ASTM*. ASTM.

Avallone, E.A., Baumeister, T. and Sadegh, A.M., 2007. *Marks’ Standard Handbook for Mechanical Engineers*. *McGraw-Hill Professional*. Vol. 1.

Bandeira, A.A., Guimarães, C.D., Freitas, L.A., and Santos, L.M., 2010. “Optimization Algorithms Applied to Nonlinear Structural Systems Solution with Constrains: A Boarding Using a Penalty Method and an Augmented Lagrangian Method” (in Portuguese). *Exacta* 8 (3): 345–61.

Chung, P.C., Cragnolino, G., and MacDonald, D.D., 1985. “Instrumented Loading Devices for Monitoring Environmentally Assisted Crack Growth in High Temperature Aqueous Systems.” *Corrosion* 41 (3): 179–83.

Chung, P., Yoshitake, A., Cragnolino, G., and MacDonald, D.D., 1985. “Environmentally Controlled Crack Growth Rate of AISI 304 Stainless Steel in High Temperature Sulfate Solutions.” *Corrosion* 41 (3): 159–68.

NAS, 2021. “North American Stainless - Long Products Stainless Steel Grade Sheet: AISI 630 / UNS S17400 / EN 1.4542.” North American Stainless.

Telega, J.J., and Gałka, A., 2001. “Augmented Lagrangian Methods for Contact Problems, Optimal Control and Image Restoration.” In *From Convexity to Nonconvexity. Nonconvex Optimization and Its Applications, 55, 311–332.*, edited by R.P. Gilbert, P.D. Panagiotopoulos, and P.M. Pardalos. Boston: Springer.

Tjayadi, L., Kumar, N., and Murty, K.L., 2020. “Accelerated Crack Growth Experiments of SS304H for Dry Storage Canister in Substitute Ocean Water – Effect of Temperature.” *Materials Today Communications* 23.

Vallourec, 2021. “Solutions for the Oil and Gas Market.” Vallourec.

Vigilante, G., Underwood, J., and Crayon, D., 2000. “Use of the Instrumented Bolt and Constant Displacement Bold-Loaded Specimen to Measure In-Situ Hydrogen Crack Growth in High-Strength Steels.” *Fatigue and Fracture Mechanics* 30: 377–87.

Vilela, P.M.L., 2016. *Modeling of Screw Connections by the Finite Elements Method* (in Portuguese). Master’s Thesis, Graduate Program in Structural Engineering, Federal University of Minas Gerais, Belo Horizonte, Brazil.

Vilela, P.M.L., Carvalho, H., Grilo, L.F., Montenegro, P.A., and Calçada, R.B., 2019, “Unitary Model for the Analysis of Bolted Connections Using the Finite Element Method,” Eng. Fail. Anal., 104(June), pp. 308–320.

7. RESPONSIBILITY NOTICE

The authors are the only responsible for the printed material included in this paper.